

## Computational Study of Anatomical Risk Factors in Idealized Models of Type B Aortic Dissection

S. Ben Ahmed <sup>a,b,e</sup>, D. Dillon-Murphy <sup>c,e</sup>, C.A. Figueroa <sup>a,c,d,\*</sup>

<sup>a</sup> Department of Surgery, University of Michigan, Ann Arbor, MI, USA

<sup>b</sup> CHU Clermont-Ferrand, Department of Vascular Surgery, F63003 Clermont-Ferrand, France

<sup>c</sup> Division of Imaging Sciences and Biomedical Engineering, King's College London, London, UK

<sup>d</sup> Department of Biomedical Engineering, University of Michigan, Ann Arbor, MI, USA

### WHAT THIS PAPER ADDS

False lumen (FL) pressure in type B aortic dissection (AD) plays an important role in aortic enlargement, but its clinical assessment is challenging and invasive. Furthermore, numerous anatomical risk factors have been identified as potential determinants of FL hemodynamics. However, the individual impact of each anatomical risk factor is poorly understood. The role of different anatomical risk factors in AD has been systematically examined using computational fluid dynamics in 14 different idealized computer models. Identical inflow and outflow boundary conditions were kept for all models. This approach enabled the quantification of the specific impact of each anatomical risk factor.

**Objective/Background:** Several risk factors have been identified in type B aortic dissection (TBAD), namely tear size, location, patency and number, and false lumen (FL) location. However, the individual impact of each of these factors is poorly understood. The impact of these factors was investigated using computational fluid dynamics (CFD).

**Methods:** Fourteen idealized models of chronic TBAD were created of different shapes (straight vs. curved vessels), different number of proximal and distal tears, tear size (4, 10, and 20 mm diameter) and shape (circular or elliptical), FL location (inner or outer arch), treated (stented), and untreated. All models had identical length, relative size of true lumen (TL) and FL, and inlet (flow) and outlet (pressure) boundary conditions. Using validated CFD tools, inlet mean pressure (MP), pulse pressure (PP), TL and FL pressures, velocities, and flows were computed for each model.

**Results:** AD increased PP and MP relative to undissected aorta. Curvature did not change pressure and flow ratio between TL and FL. Inner curvature FL showed slightly larger pressures and tear velocities. Larger tears decreased hemodynamic differences between TL and FL. The combination of proximal and distal tear size determines the overall hemodynamics: larger proximal tears increased FL PP by up to 76%. Conversely, larger distal tears decreased FL PP and MP. Large proximal and distal tears decreased tear velocity (by up to 65%) and increased FL flow (up to 12 times). Proximal tear stenting resulted in a 54% reduction of PP. Conversely, distal occlusion tear increased FL PP and MP by 144% and 7%, respectively.

**Conclusion:** Unfavorable hemodynamic conditions such as larger FL pressure occur when distal tear is small or absent, proximal tears are large, and FL is at the inner curvature, in agreement with previous clinical studies. CFD analysis is a powerful tool to understand the interplay between anatomy and hemodynamics in TBAD.

© 2016 European Society for Vascular Surgery. Published by Elsevier Ltd. All rights reserved.

Article history: Received 18 December 2015, Accepted 19 July 2016, Available online XXX

**Keywords:** Aortic disease, Computational fluid dynamics, Computer model, False lumen, Hemodynamics, Predictors

### INTRODUCTION

Type B aortic dissection (TBAD) is a life-threatening disease involving the descending aorta. Patient management is challenging and prognosis poor, with a high 3-year mortality (10–25%).<sup>1,2</sup> In chronic TBAD, the 5-year survival rate is 60–80% for medical management, 77.7–84.4% for thoracic endovascular aneurysm repair (TEVAR), and 68–92% for open surgery.<sup>3</sup> Aneurysmal expansion and rupture are the major complications.

<sup>e</sup> S. Ben Ahmed and D. Dillon-Murphy contributed equally to this work.

\* Corresponding author. Computational Vascular Biomechanics Lab, North Campus Research Complex, 2800 Plymouth Road, Building 20 – 211 W, Ann Arbor, MI 48109, USA.

E-mail address: [figueroa@med.umich.edu](mailto:figueroa@med.umich.edu) (C.A. Figueroa).

1078-5884/© 2016 European Society for Vascular Surgery. Published by Elsevier Ltd. All rights reserved.

<http://dx.doi.org/10.1016/j.ejvs.2016.07.025>

There are numerous TBAD anatomical predictors of long-term complications. However, the mechanisms behind aortic growth are poorly understood. Studies have identified risk factors such as false lumen (FL) location in the aortic curvature, number and size of intimal tears,<sup>4-8</sup> tear patency,<sup>4</sup> and location,<sup>6</sup> and FL patency.<sup>9,10</sup> Absence or occlusion of distal tears leads to elevated pressures,<sup>5,8</sup> FL partial thrombosis, and aortic growth.<sup>9,10</sup> FL hemodynamics seem to play an important role in aneurysmal complications but are difficult to measure clinically. The numerous factors determining FL hemodynamics make it difficult to perform systematic comparisons between patients.

Computational fluid dynamics (CFD) is a tool that enables detailed and controlled hemodynamic investigation. The aim of this study was to perform a systematic study of hemodynamic alterations associated with morphological

predictors of aortic growth using CFD in a series of idealized computer-aided design (CAD) TBAD models.

**METHODS**

Fourteen idealized aortic CAD models featuring a true lumen (TL), a FL, and a maximum of two tears were made. The models included variations in shape (curvature), FL position relative to the aortic curvature, number, size, and patency of tears relative to a baseline geometry (Fig. 1). All models were built with TL and FL of equal lengths and diameters. This approach enabled a controlled comparison among models, as only one geometrical factor differed at a time. Total aortic length and diameter were 500 mm and 25 mm, respectively. The FL and TL lengths were 250 mm and their equivalent diameters 32 mm and 9 mm, respectively. The septum was 1 mm thick. The stented model had

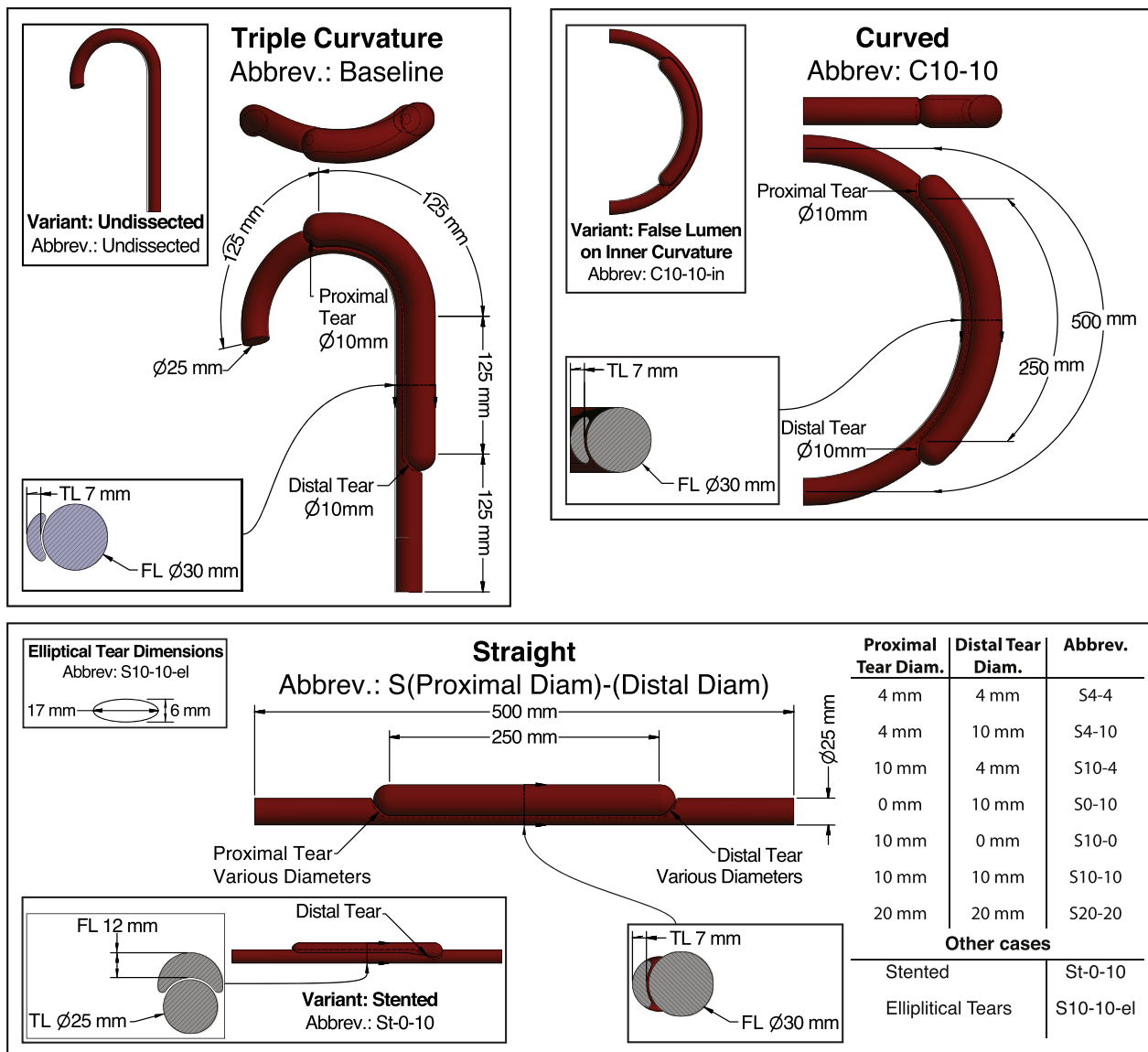


**Figure 1.** Schematic of the aortic dissection models, including shape, false lumen location relative to the curvature, length, and diameter, and abbreviated names. Top left: triple-curved models. Top right: curved models. Bottom: straight models. *Note.* Abbrev. = abbreviated name; TL = true lumen; FL = false lumen; ø = diameter; diam = diameter.

larger TL (25 mm diameter) and narrower FL (9 mm equivalent diameter) in the first three-quarters of the dissection, where the stent was placed. An image of each model is shown in Fig. 1. The baseline model has three curvatures in the sagittal, transverse, and coronal planes, mimicking a human aorta,<sup>11</sup> with the FL arbitrarily placed at the outer curvature. The curved model (“semi-torus” shape) in a single 180° planar curvature was constructed in two variations with the FL in the inner or outer side of the arch. Tears were circular for most models, with diameters of 4, 10, and 20 mm. One model was created with elliptical tears, rendering an equivalent area to a 10 mm circular tear. A nondissected model was also created based on the shape of the baseline model.

CFD analysis was performed using the validated Finite-Element code “CRIMSON”<sup>12</sup> at the High-Performance Computer Cluster of the University of Michigan. Finite element tetrahedral meshes were iteratively refined until mesh-independent results were achieved.<sup>13</sup> Mesh size ranged between  $0.12 \times 10^6$  elements (undissected model) and  $3.8 \times 10^6$  (S4-4 model). The vessel walls and septum were modeled as rigid. Blood was treated as a Newtonian and incompressible fluid with a dynamic viscosity of 4 mPa and a density of 1060 kg/m<sup>3</sup>. A pulsatile flow (mean 4 L/minute, 46 beats per minute) was prescribed at the inlet. At the outlet, a pressure waveform (120/80 mmHg) was applied by means of a three-element Windkessel model. The inlet waveform and the outlet pressure were the same in all cases in order to make consistent comparisons. A key piece of information to be gained in each analysis is the inlet pressure, which is different for each case. Inlet pressure is higher in situations where the hemodynamic alterations of the dissection are higher. Simulations were run until periodic solutions were achieved, imposing total residual tolerances for the entire mesh of  $1 \times 10^{-3}$ . Only results obtained in the last cycle are reported.

For each model, pulse pressure (PP), mean pressure (MP) and mean flow (Qm) were measured at five different locations: inlet (section A) and outlet (section E), and three sites of the dissected segment 12 cm apart from each other. These sites are referred to as prox. (section B), mid. (section C), and dist. (section D) (Figs. 2–6; Table 1). Peak velocity from TL to FL at the level of the tear (tear velocity) was also measured, as well as mid TL and FL velocity (Table 1).

## RESULTS

### *Hemodynamics in undissected and dissected aortic models*

**Pressure.** The undissected and dissected geometries were compared (Fig. 2; Table 1). Inlet PP and MP increased by 61% and 5%, respectively, in the baseline-dissected model compared with the undissected. The TL experienced larger gradients in PP (63% drop) and MP (5% drop) compared with the undissected model (41% drop in PP and nearly constant MP). Conversely, the FL showed constant PP and MP throughout its length: these values are higher than in the undissected case. The difference in PP between the FL

and the undissected case varied between 7 mmHg (proximal) and 24 mmHg (distal). MP between the FL and the undissected case is nearly constant (2 mmHg, Table 1).

**Mean flow and velocity.** A 78%:22% TL:FL flow split was found in the baseline model. Mid-TL and FL velocities were, respectively, 2.7 times faster and 4.3 times slower in the dissected model than in the undissected model. Large peak systolic velocities were observed at the proximal and distal tears (Table 1).

In summary, dissection resulted in increased inlet PP and MP, and large TL PP and MP gradients. These alterations can be explained by the increased resistance introduced by the dissected channel (FL).

### *Impact of curvature and FL location*

**Curvature.** The hemodynamic differences between baseline, curved, and straight dissection models were investigated (Fig. 3; Table 1), with the goal of assessing the impact of curvature. All models had proximal and distal tears of 10 mm diameter.

**Pressure.** All models showed similar pressure waveforms, PP, and MP in both TL and FL. Differences in inlet PP and MP between the straight and the baseline cases were 4% and 0.4%, respectively (Table 1).

**Mean flow and velocity.** An 80%:20% TL:FL flow split was found in all models (Table 1). Mid-TL velocities were similar in all cases (range 267–283 cm/second) (Table 1). Mid-FL velocities were much smaller and similar in range among cases (range 23–36 cm/second). Large peak systolic velocities were observed at proximal and distal tears.

In summary, curvature did not significantly change PP, MP, and flow ratios between TL and FL.

**Impact of FL location.** The impact of FL location was assessed relative to the arch (Fig. 3; Table 1) by comparing two models: C10-10-in (inner curvature FL) and C10-10 (outer curvature FL).

**Pressure.** Both models showed similar PP and MP in TL and FL (Fig. 3). C10-10-in showed larger inlet-PP (7.5%) and inlet-MP (0.4%) compared with C10-10. C10-10-in showed slightly larger gradients in TL-PP (67% drop) relative to C10-10 (65% drop). C10-10-in FL showed a 4% higher PP and virtually identical MP (Table 1).

**Mean flow and velocities.** An 80%:20% TL:FL flow split was found in both models. Mid-TL and FL velocities were 4% faster and 15% slower, respectively, in the C10-10-in. Peak systolic tear velocities were 4% larger in C10-10-in (Table 1).

In summary, FL location in the aortic curvature did not have a large impact on hemodynamics. There was, however, a trend of larger PP, MP, and tear velocities when the FL was on the inner curvature. Similar patterns were found for models with 4-mm connecting tears (Table 1).

### *Impact of tear size: proximal and distal tears of equal size*

Straight models with 4-, 10-, and 20-mm diameter tears, both proximally and distally (Fig. 4; Table 1), were investigated.

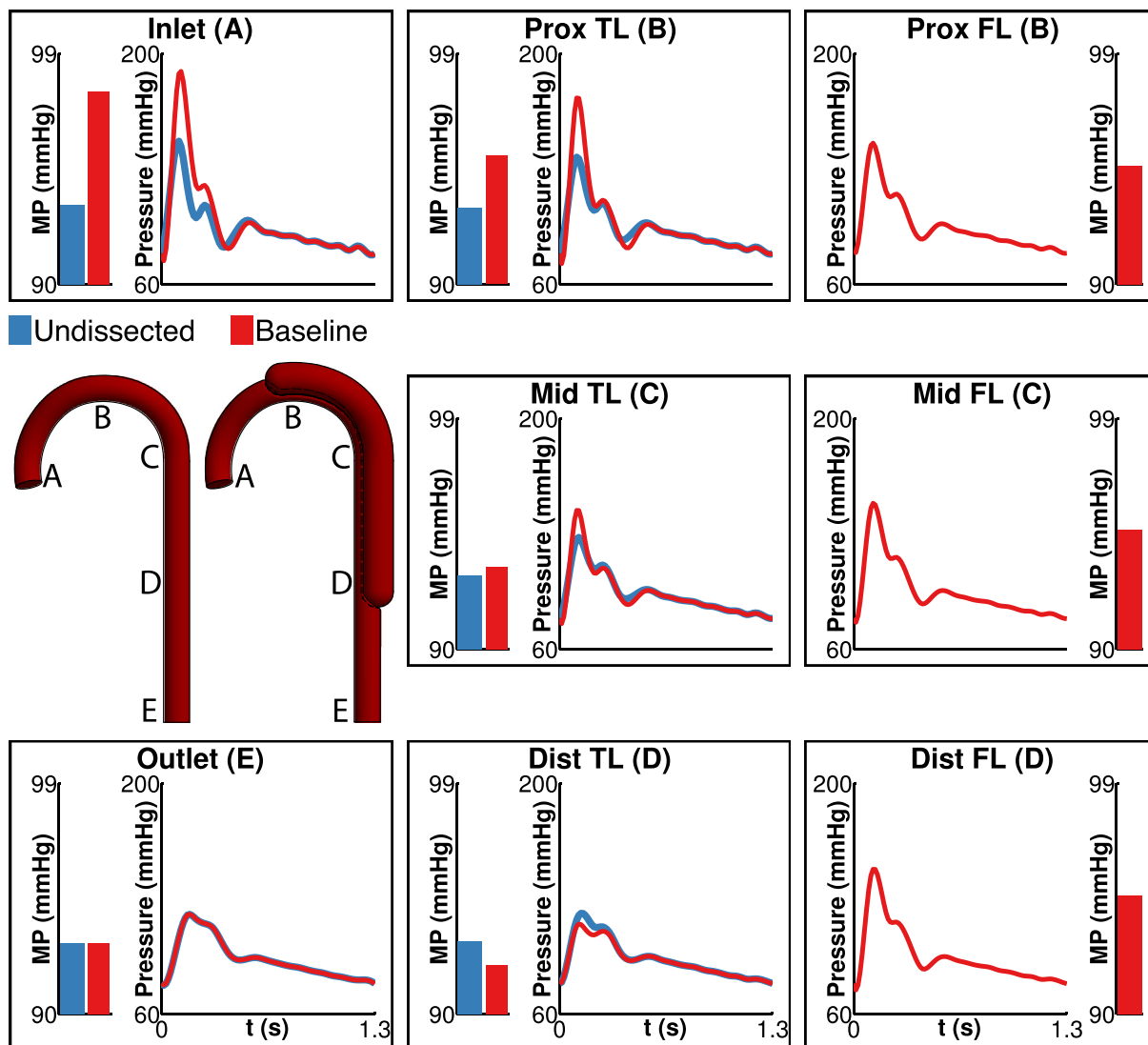


**Figure 2.** Hemodynamics in undissected and dissected aortic models. Middle left: schematic of the undissected and baseline dissected models and location of reported pressures in the true lumen (TL) and false lumen (FL) (A–E). Each box shows the mean pressure (MP) in a bar plot and the pressure waveforms at the inlet, along the TL and FL, and at the outlet. Pressures are reported at: the inlet (inlet [A]), proximal region of the TL (Prox TL [B]), proximal region of the FL (Prox FL [B]), middle region of the TL (Mid TL [C]), middle region of the FL (Mid FL [C]), distal region of the TL (Dist TL [D]), distal region of the FL (Dist FL [D]), and at the outlet (Outlet [E]).

**Pressure.** Inlet pressures were greatly affected by tear size. Compared with S20-20, S4-4 had larger inlet PP (176%) and inlet MP (7%) (Table 1). FL MP was constant in all models. S4-4 had the largest FL PP and FL MP.

**Mean flow and velocities.** TL:FL flow splits were greatly affected by tear size: 95%:5%, 81%:19%, and 33%:67%. TL:FL ratios were obtained for the S4-4, S10-10, and S20-20, respectively. Mid-FL velocities were largest in S20-20. Conversely, S4-4 showed the largest TL velocities. S20-20 showed the smallest peak systolic tear velocities (three times slower than the S4-4). Fig. 4 also shows significant differences in flow waveforms between lumina. Larger connecting tears resulted in increased early diastole FL backflow. In summary, large tears decreased hemodynamic differences between TL and FL, and resulted in smaller inlet MP and inlet PP.

**Impact of tear shape.** Two models with identical tear areas ( $0.78 \text{ mm}^2$ ) but different shapes were investigated: circular with 10-mm diameter versus elliptical (Fig. 4; Table 1). Results showed negligible hemodynamic differences.

#### **Impact of the tear size: proximal and distal tear of different sizes**

Four straight models with different proximal and distal tear sizes of 4 and 10 mm were considered (Fig. 5; Table 1): S10-10, S4-4, S4-10, and S10-4.

**Pressure.** The S10-10 and S4-4 models were adopted as references, and the impact of increasing or decreasing proximal and distal tear sizes was investigated (Fig. 5; Table 1).

**Changes relative to S10-10.** Introducing a single, smaller 4-mm tear changed the hemodynamics noticeably: inlet and

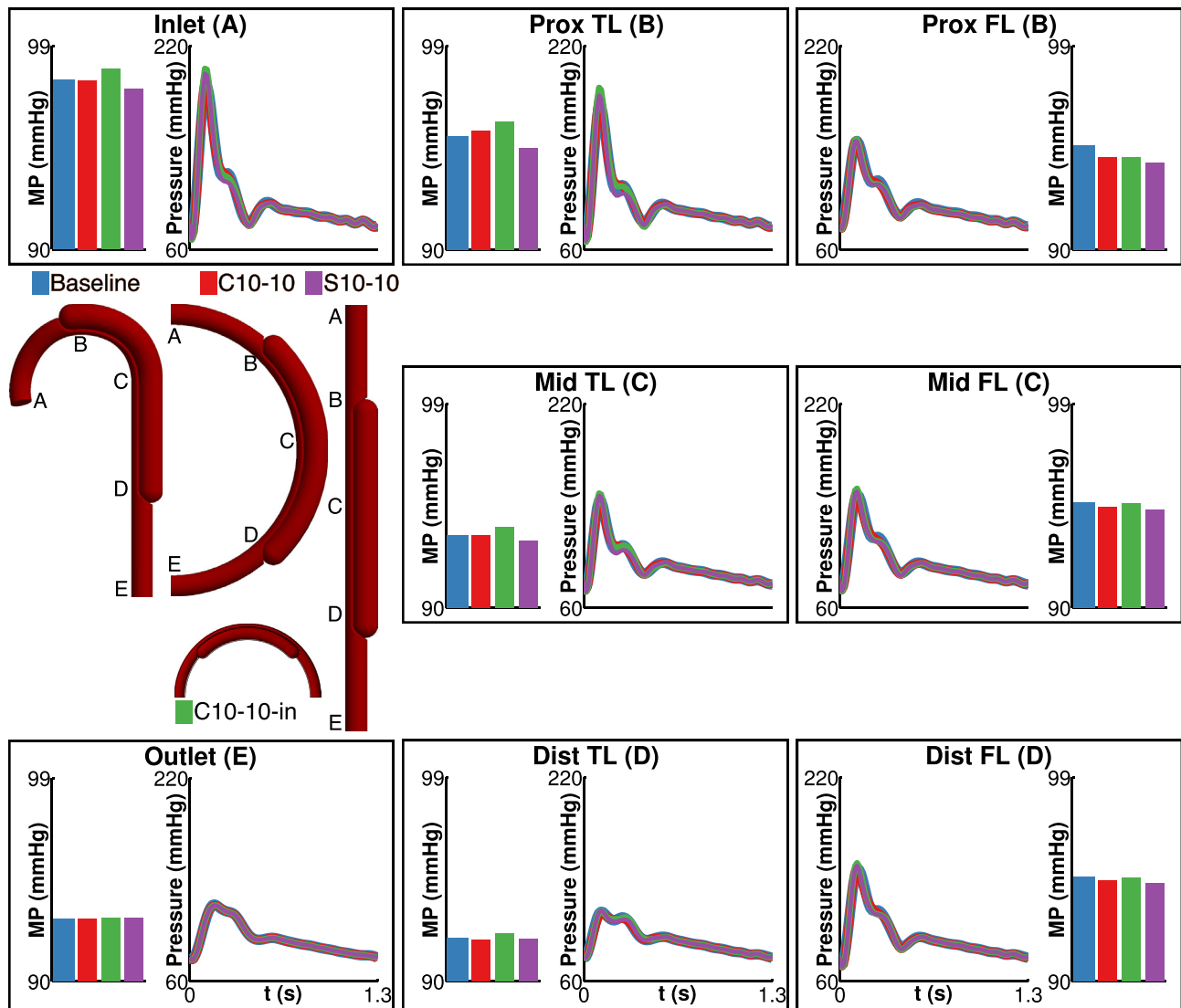


**Figure 3.** Impact of curvature and FL location. Middle left: schematic of the undissected and baseline dissected models and location of reported pressures in the true lumen (TL) and false lumen (FL) (A–E). Each box shows the mean pressure (MP) in a bar plot and the pressure waveforms at the inlet, along the TL and FL, and at the outlet. Each box shows the mean pressure (MP) in a bar plot and the pressure waveforms at the inlet, along the TL and FL, and at the outlet. *Note.* See Fig. 2 for the key.

TL pressures increased. FL experienced large increases in PP and MP in S10-4. Conversely, FL-PP and FL-MP decreased when proximal tear size was reduced (S4-10).

**Changes relative to S4-4.** Changing the size of either the proximal or the distal tear did not modify inlet and TL pressures noticeably. However, FL alterations were noticeable: increasing proximal tear size (S10-4) increased PP and MP. Conversely, increasing the distal tear size (S4-10) decreased FL-PP and FL-MP.

**Mean flow and velocities.** TL:FL flow splits were different between all models: S10-4 and S4-10 had identical splits (93%:7%), S4-4 had a 95%:5% split, and S10-10 a 81%:19% split. Mid-TL velocities were highest in the S4-4 (391 cm/second) and smallest in the S10-10 (283 cm/second). Large peak systolic velocities were observed at the small tear of S10-4 and S4-10 (1.4 times faster than the S4-4; Table 1). In summary, larger distal tears decreased FL PP and FL MP,

whereas smaller distal tears increased FL PP and FL MP. Conversely, larger proximal tears increased FL PP and FL MP, whereas smaller proximal tears decreased FL PP and FL MP. Large tears decreased tear velocity, whereas small tears increased it.

#### Impact of tear patency

The impact of tear patency was investigated in four models: patent tears (S10-10), distal tear occlusion (S10-0), proximal tear occlusion (S0-10), and stented proximal tear (St-0-10) (Fig. 6).

**Pressure.** Inlet pressures were highest in models with one occluded tear (S10-0 or S0-10), where all flow is forced through the TL. St-0-10 showed the smallest inlet pressures, showing that proximal tear occlusion and TL expansion result in favorable hemodynamics. FL pressures showed large differences: S10-0 had the largest PP and MP (167 and

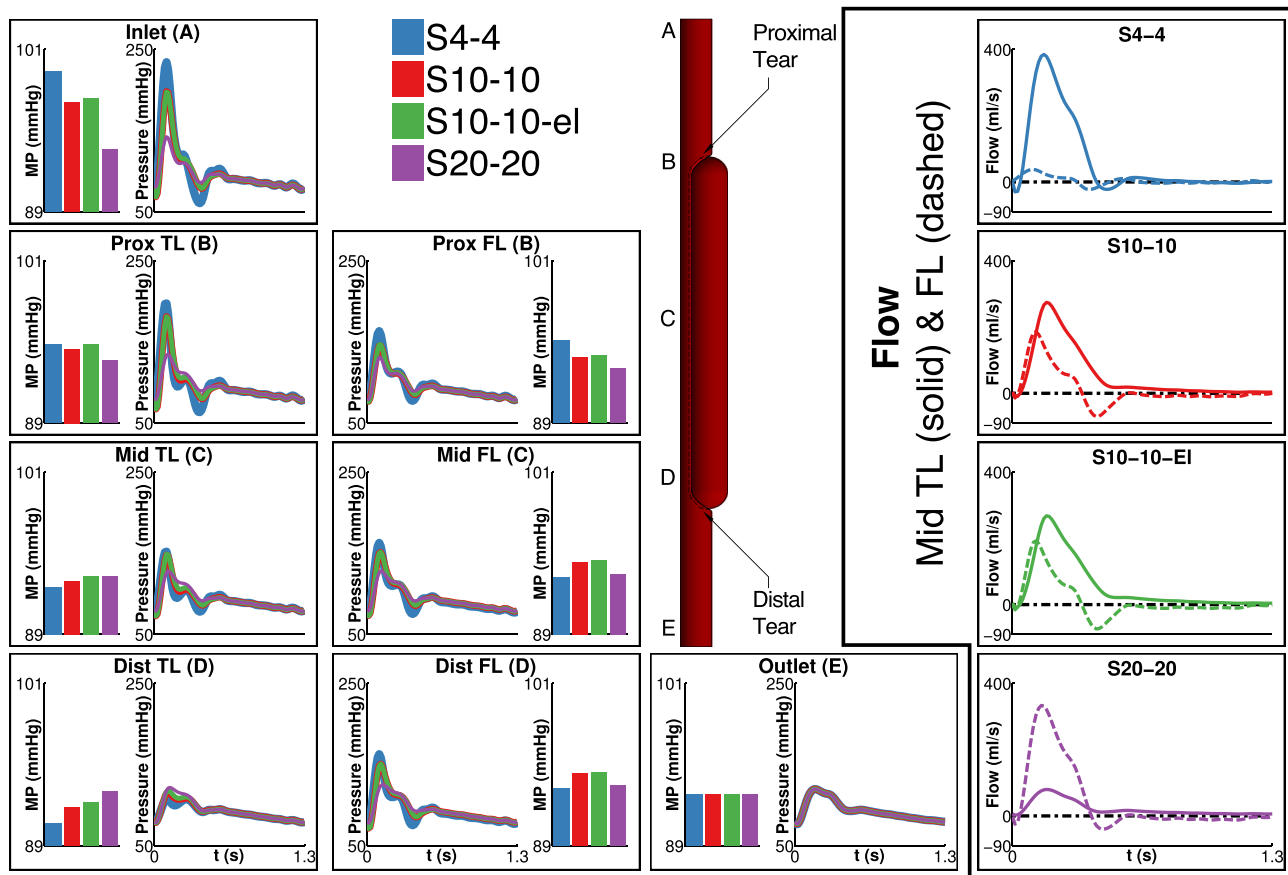


**Figure 4.** Impact of tear size: proximal and distal tears of equal size. Schematic of the S4-4, S10-10, S10-10-el, and S20-20 models with location of reported pressures in the true lumen (TL) and false lumen (FL) (A–E). Each box shows the mean pressure (MP) in a bar plot and the pressure waveforms at the inlet, along the TL and FL, and at the outlet. Right panel: flows in the TL (solid line) and FL (dashed line) in the mid-section of the models (C). Larger connecting tears result in larger FL flows. Maximum early diastole FL backflow was obtained for the models with 10-mm connecting tears. *Note.* See Fig. 2 for the key.

101 mmHg, respectively). St-0-10 had the smallest PP (31 mmHg) and MP (91 mmHg).

**Mean flow and velocities.** Single-tear models showed near-zero FL flow. S0-10 and S10-0 showed faster mid-TL velocity, whereas St-0-10 presented slower mid-TL velocity, compared with S10-10 (Table 1). In summary, proximal tear occlusion via stenting decreased PP, MP, flow, and velocity. Narrowed TL in the presence of a single tear increased TL PP and velocity. Distal tear occlusion increased FL-PP, FL-MP, and TL velocity.

## DISCUSSION

TBAD presents with large anatomical variability: lengths, TL:FL area ratios, number of tears, and so on. Aortic dissection hemodynamics are the result of interactions between these factors. Computational modeling can help to elucidate the role of each factor. CFD tools were used to investigate hemodynamics in 14 idealized AD models with different curvatures, tear size, number of tears, and tear patency. In all cases, identical inlet and outlet conditions were applied. This enabled a systematic comparison between models.

The findings revealed that curvature and tear shape had little impact on the hemodynamics. Therefore, most of the

analyses were performed using straight dissections with circular tears.

## Pressure

FL growth and aortic rupture is one of the major complications of TBAD. Pressure has been hypothesized to be a determinant of FL growth. Changes in both MP and PP likely play a significant role in this process.<sup>9</sup> According to Laplace's law, an increase in FL MP and reduction in FL wall thickness following dissection increases mean wall stress relative to its predissection value. As wall stress increases, FL diameter and risk of rupture increase. Therefore, gain in FL MP and FL PP directly affect FL wall stress, diameter enlargement, and risk of rupture.

Recent animal studies have identified the strong role of PP in aortic remodeling,<sup>14,15</sup> specifically wall thickening, stiffening, and loss of axial tension. It is because of these findings that PP was systematically reported. In general, PP was seen to be more affected by dissection than MP (Figs. 2–6; Table 1). Increases in MP and PP are directly attributable to the FL, which increases the flow resistance substantially, particularly at peak systole.

All computations had uniform outlet pressure and inlet flow conditions. Even with a fixed inlet flow, we obtained different inlet pressures due to the different afterloads

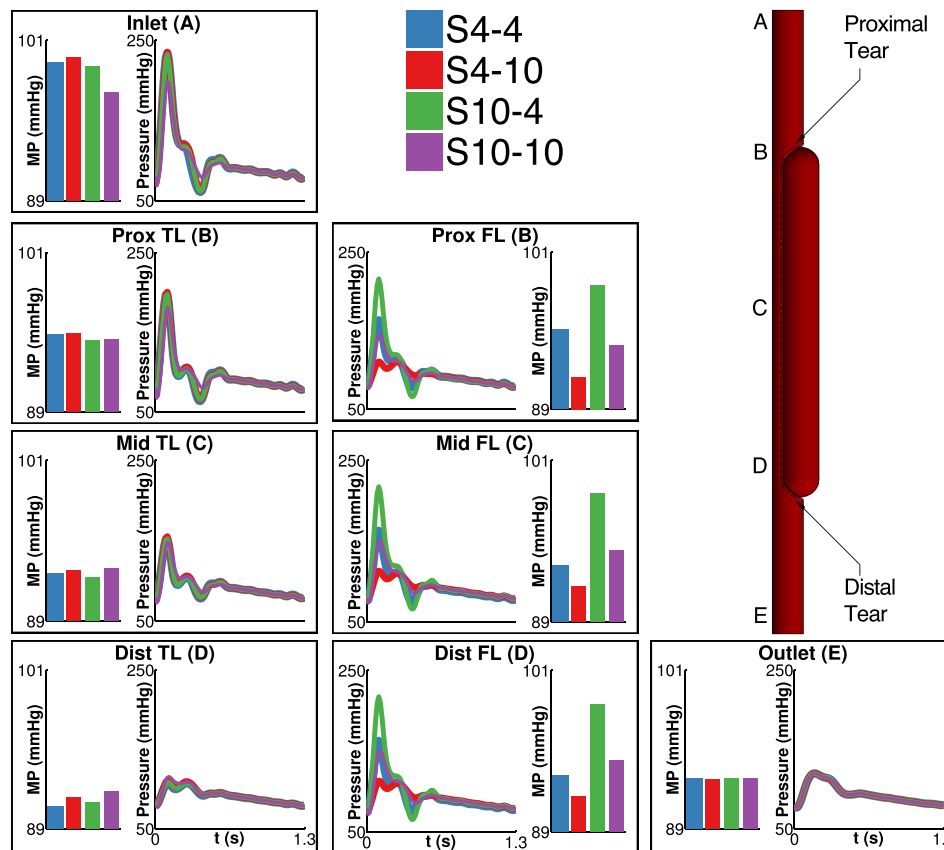


**Figure 5.** Impact of tear size: proximal and distal tears of different sizes. Top right: schematic of the S4-4, S4-10, S10-4, and S10-10 models with location of reported pressures in the true lumen (TL) and false lumen (FL) (A–E). Each box shows the mean pressure (MP) in a bar plot and the pressure waveforms at the inlet, along the TL and FL, and at the outlet. *Note.* See Fig. 2 for the key.

(e.g., resistances) of each model. In a clinical setting, however, the heart may not be able to adjust to large changes in afterload and reductions in cardiac output may occur.

### Flow and velocity

TL and FL flow splits and tear velocity are greatly affected by tear size. Small tears decreased FL flow and velocity. The opposite trend was found for large tears. These findings are consistent with those reported by Rudenick et al.<sup>8</sup>

### Previous clinical studies

Primary proximal tear located at the inner curvature has been identified as a predictor of complicated acute TBAD in Weiss et al.<sup>16</sup> and Loewe et al.<sup>17</sup> Tolenaar et al.<sup>18</sup> showed that FL location at the outer curvature is associated with decreased aortic growth. Therefore, it appears that inner aortic arch FL location is associated with more adverse hemodynamics. The present results corroborated these findings (Fig. 3). Larger MP, PP, and lower velocities were found in the FL when this was located at the inner curvature.

The present study showed that it is the combination of proximal and distal tear size that determines FL hemodynamics. For a given distal tear size, larger proximal tears increased FL pressure. This agrees with the studies of Evangelista et al.,<sup>6,7</sup> which showed that proximal tear size

$\geq 1$  cm was a predictor of aortic growth. Conversely, for a given proximal tear size, larger distal tears decreased FL pressure, whereas smaller or absent distal tears resulted in FL pressure increase. These results are consistent with clinical studies that identified FL partial thrombosis as a predictor of aortic growth<sup>10,19,20</sup> and mortality.<sup>9</sup> The current results were also in agreement with experimental studies,<sup>5,8</sup> which showed that TL and FL pressure equilibrates as tear size increases. The lack of compliance of the models explains why no increase in FL diastolic pressure in the absence of the distal tear was found; however, a 16% drop was found, as described by Tsai et al.<sup>21</sup> and Rudenick et al.<sup>8</sup>

TEVAR is one of the treatments for TBAD. Covering the proximal tear aims to restore TL size and to induce FL thrombosis.<sup>22</sup> Two models with proximal tear occlusion were investigated (S0-10, St-0-10), which revealed large decreases in FL pressure, velocity, and flow. This is consistent with thrombus formation (due to slower blood velocity) and positive aortic remodeling (due to smaller FL pressure).

### Limitations

This study has several limitations. The vessel walls were assumed rigid. In the patient-specific study performed by Dillon-Murphy et al.<sup>23</sup> it was demonstrated that rigid wall analysis overpredicts the pulsatility of both pressure and flow waveforms. While differences in mean values between

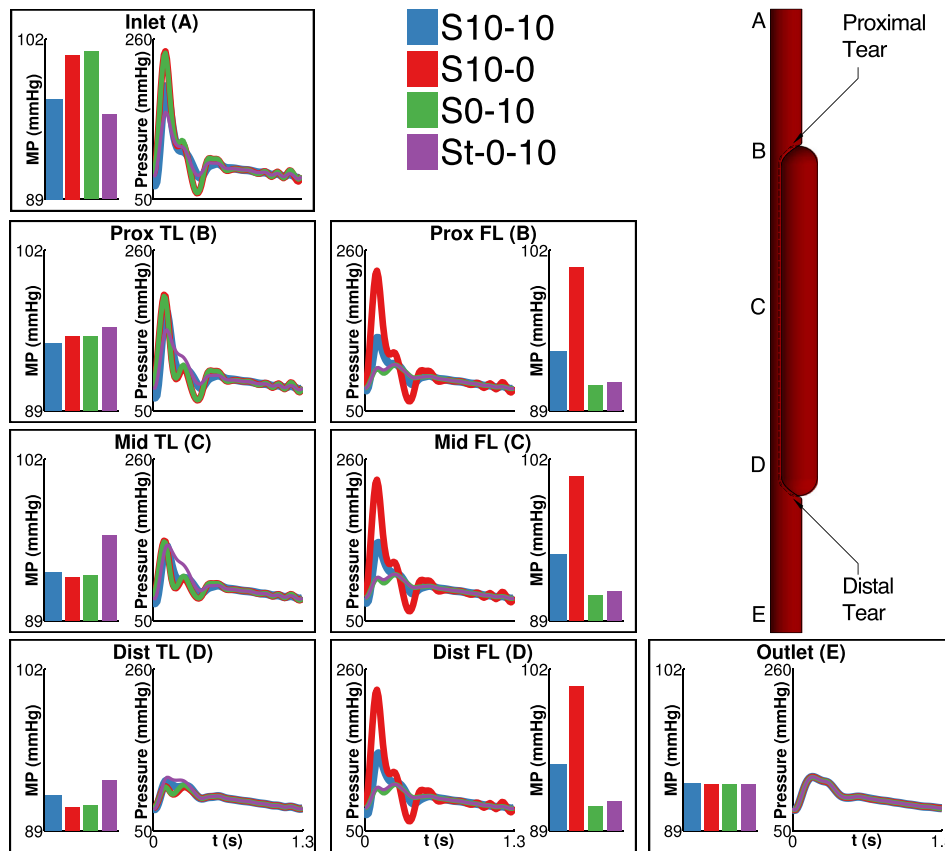


**Figure 6.** Impact of tear patency. Top right: schematic of the S10-10, S10-0, S0-10, and St-0-10 models with location of reported pressures in the true lumen (TL) and false lumen (FL) (A–E). Each box shows the mean pressure (MP) in a bar plot and the pressure waveforms at the inlet, along the TL and FL, and at the outlet. *Note.* See Fig. 2 for the key.

rigid and compliant analysis was small, the difference in pulsatility was up to 50% in some cases. This difference will be larger in more compliant aortas. A rigid wall model might be a reasonable assumption to study chronic TBAD, where aortic wall and dissection septum are stiffer.

The idealized models had a maximum of two tears, while patients with aortic dissection usually have more than two.<sup>24</sup> Size and tear number affect flow transfer between lumina, and therefore pressure. Thus, each presentation of AD has its own particular hemodynamics.

The models did not include side branches, while in most cases several vessels arise from both TL and FL. Flow to side branches makes the velocity in AD more complex.<sup>25</sup> This may result in areas of slow flow (and therefore more likely to thrombose), pressure alterations, and so on. The septum was not helical, as is usually the case in TBAD. A more complex septum configuration will affect velocity and pressure in TL and FL. Lastly, the models had a constant TL:FL area ratio (0.175), except in the stented model (1.485). Models with different area ratios are likely to show substantial differences in hemodynamics. Recently, Lavingia et al.<sup>26</sup> showed that aortic growth rate and need for intervention was higher in patients with TL:FL volume ratio <0.8.

In summary, most of the limitations emanate from the simplicity of the idealized models. CFD analysis in patient-specific TBAD models can produce detailed insight into

the complex hemodynamics of that particular patient.<sup>23</sup> However, it is not easy to assess the individual impact of all the anatomical factors known to play a role in TBAD. It is through the study of simplified models that the relative value of these anatomic variations can be understood.

### Conclusions

CFD enables systematic investigation of anatomical determinants of TBAD hemodynamics. Unlike clinical studies in which a single factor is investigated, computational analysis enables parametric approaches such as those presented here.

The results highlight the large alterations in PP induced by the septum. Most previous studies focused on MP changes but had neglected PP, a metric linked to significant aortic remodeling.<sup>14,15</sup> It is also highlighted that FL pressure is the result of the interplay between multiple parameters, mostly entry and exit tear sizes. Therefore, FL pressure cannot be assessed by a single parameter such as proximal tear size: for a given proximal tear size, different distal tear sizes result in different FL pressures. Several anatomical factors play a role in FL hemodynamics. In this study, distal tear occlusion and a large proximal tear were the most relevant geometrical parameters. Both were associated with the highest FL pressure increases. The study provides a range of idealized cases that clearly illustrate hemodynamics in AD. Although the focus of this work was TBAD,

**Table 1.** Mean flow in the true lumen (TL) and false lumen (FL), velocities (cm/second) at proximal and distal tears and in the middle of the TL and FL, mean pressures (MP; mmHg) and pulse pressures (PP; mmHg) at the inlet and along the TL and FL. Percentages refer to fraction of total flow in the dissection.

Models	TL Qm (%)	FL Qm (%)	V Prox Tear	V Dist Tear	V Mid TL	V Mid FL	Inlet MP	Prox TL MP	Prox FL MP	Mid TL MP	Mid FL MP	Dist TL MP	Dist FL MP	Inlet PP	Prox TL PP	Prox FL PP	Mid TL PP	Mid FL PP	Dist TL PP	Dist FL PP
Undissected					101	101	93.7	93.0		92.9		92.8		71.1	58.3		48.2		41.5	
Baseline	78	22	217	214	272	23	98.3	95.0	94.6	93.2	94.7	91.9	94.6	114.9	98.3	66.5	68.1	69.1	34.6	67.5
C4-4	95	5	298	299	376	7	101.3	96.2	95.1	93.0	95.3	91.0	95.2	168.2	129.2	82.2	70.9	83.2	28.5	83.1
C4-4-in	95	5	308	307	392	6	102.0	97.6	96.4	93.8	95.9	92.3	96.5	182.6	141.3	86.0	76.5	87.7	34.4	87.7
C10-10	80	20	225	225	272	30	98.3	95.3	94.1	93.2	94.5	91.8	94.4	115.6	100.3	66.2	65.1	68.7	31.6	66.9
C10-10-in	81	19	235	235	281	26	98.6	95.7	94.1	93.6	94.6	92.1	94.6	124.3	108.8	67.0	69.9	72.2	34.6	70.4
S4-4	95	5	302	300	391	6	100.6	94.8	95.1	93.8	94.9	90.7	93.2	175.6	129.5	83.5	76.5	84.7	28.3	84.9
S4-10	93	7	420	67	381	7	100.6	94.9	91.5	92.8	91.7	91.4	91.6	174.0	131.4	30.9	75.8	33.3	31.4	33.4
S10-4	93	7	67	421	380	7	100.0	94.4	98.5	92.3	98.6	91.0	98.5	171.5	128.3	147.3	73.0	148.8	28.8	149.6
S10-10	81	19	228	227	283	36	97.8	94.5	93.8	92.9	94.3	91.9	94.3	119.8	101.6	65.8	68.1	70.3	34.9	68.8
S10-10-el	82	18	222	217	276	30	98.0	94.8	94.0	93.3	94.5	92.2	94.4	120.0	101.4	67.0	69.0	70.4	37.1	68.9
S10-0	100	0	0		416	0	97.4	95.0	100.6	92.5	100.6	90.9	100.6	186.0	134.5	166.6	74.8	166.6	28.5	166.6
S0-10	100	0	0		417	0	101.5	95.1	91.0	92.7	91.0	91.0	91.0	185.5	131.7	30.8	73.1	30.8	30.3	30.7
St-0-10	100	0		0	90	0	96.3	95.8	91.3	95.9	91.3	93.1	91.3	85.5	75.7	31.1	65.7	31.1	38.4	31.1
S20-20	33	67	105	105	87	48	94.1	93.6	93.1	93.3	93.5	93.1	93.5	63.7	54.0	51.3	46.0	46.3	41.1	44.7

Note. For each model, the C, S, or St referred to the shape of the model: C = curved, S = straight, St = stented (Fig. 1). The first number referred to the diameter of the proximal tear: 0, 4, 10, or 20 mm. The second number referred to the diameter of the distal tear: 0, 4, 10, or 20 mm. "el" referred to the elliptical shape of proximal and distal tears rendering an equivalent area to a 10-mm circular tear. In the curved model, "in" referred to the location of the FL at the inner curvature and if "in" was not mentioned, the FL was located at the outer curvature. TL Qm = mean flow in the TL; FL Qm = mean flow in the FL; V = velocity; Prox Tear = proximal tear; Dist Tear = distal tear; Mid-TL = middle of the TL; Mid-FL = middle of the FL; Prox TL = proximal part of the TL; Prox FL = proximal part of the FL; Dist TL = distal part of the TL; Dist FL = distal part of the FL.

the anatomical situations presented here are also applicable to cases of repaired type A with chronic type B component. It may help clinicians in understanding the hemodynamic conditions that a patient is likely to have based on similar anatomical characteristics to the cases studied here.

#### ACKNOWLEDGMENTS

The authors acknowledge the French Society of Vascular Surgery and the Frankel Cardiovascular Center of the University of Michigan. The authors also acknowledge Professors Ramon Berguer and David M. Williams, and Dr. Paula Rudenick for their assistance and feedback.

#### CONFLICTS OF INTEREST

None.

#### FUNDING

The authors acknowledge the European Research Council/ERC Grant Agreement No. 307532.

#### REFERENCES

- Steuer J, Eriksson M-O, Nyman R, Björck M, Wanhainen A. Early and long-term outcome after thoracic endovascular aortic repair (TEVAR) for acute complicated type B aortic dissection. *Eur J Vasc Endovasc Surg* 2011;**41**:318–23.
- Tsai TT, Fattori R, Trimarchi S, Isselbacher E, Myrmet T, Evangelista A, et al. Long-term survival in patients presenting with type B acute aortic dissection insights from the International Registry of Acute Aortic Dissection. *Circulation* 2006;**114**:2226–31.
- Fattori R, Cao P, De Rango P, Czerny M, Evangelista A, Nienaber C, et al. Interdisciplinary expert consensus document on management of type B aortic dissection. *J Am Coll Cardiol* 2013;**61**:1661–78.
- Tolenaar JL, van Keulen JW, Trimarchi S, Jonker FHW, van Herwaarden JA, Verhagen HJM, et al. Number of entry tears is associated with aortic growth in type B dissections. *Ann Thorac Surg* 2013;**96**:39–42.
- Berguer R, Parodi J, Schlicht M, Khanafer K. Experimental and clinical evidence supporting septectomy in the primary treatment of acute type B thoracic aortic dissection. *Ann Vasc Surg* 2015;**29**:167–73.
- Evangelista A, Salas A, Ribera A, Ferreira-González I, Cuellar H, Pineda V, et al. Long-term outcome of aortic dissection with patent false lumen predictive role of entry tear size and location. *Circulation* 2012;**125**:3133–41.
- Evangelista A, Galuppo V, Gruosso D, Cuéllar H, Teixidó G, Rodríguez-Palomares J. Role of entry tear size in type B aortic dissection. *Ann Cardiothorac Surg* 2014;**3**:403–5.
- Rudenick PA, Bijmens BH, García-Dorado D, Evangelista A. An in vitro phantom study on the influence of tear size and configuration on the hemodynamics of the lumina in chronic type B aortic dissections. *J Vasc Surg* 2013;**57**:464–74.
- Tsai TT, Evangelista A, Nienaber CA, Myrmet T, Meinhardt G, Cooper JV, et al. Partial thrombosis of the false lumen in patients with acute type B aortic dissection. *N Engl J Med* 2007;**357**:349–59.
- Trimarchi S, Tolenaar JL, Jonker FHW, Murray B, Tsai TT, Eagle KA, et al. Importance of false lumen thrombosis in type B aortic dissection prognosis. *J Thorac Cardiovasc Surg* 2013;**145**:S208–12.
- Berguer R, Kieffer E. The aortic arch and its branches: anatomy and blood flow. In: *Surgery of the arteries to the head*. New York: Springer-Verlag; 1992. p. 5–31.
- Cardiovascular Integrated Modelling and Simulation (CRIMSON)*. Available at: <http://www.crimson.software/> [accessed 17.7.15].
- Sahni O, Müller J, Jansen KE, Shephard MS, Taylor CA. Efficient anisotropic adaptive discretization of the cardiovascular system. *Comput Methods Appl Mech Eng* 2006;**195**:5634–55.
- Eberth JF, Gresham VC, Reddy AK, Popovic N, Wilson E, Humphrey JD. Importance of pulsatility in hypertensive carotid artery growth and remodeling. *J Hypertens* 2009;**27**:2010–21.
- Eberth JF, Popovic N, Gresham VC, Wilson E, Humphrey JD. Time course of carotid artery growth and remodeling in response to altered pulsatility. *Am J Physiol Heart Circ Physiol* 2010;**299**:1875–83.
- Weiss G, Wolner I, Folkmann S, Sodeck G, Schmidli J, Grabenwöger M, et al. The location of the primary entry tear in acute type B aortic dissection affects early outcome. *Eur J Cardiothorac Surg* 2012;**42**:571–6.
- Loewe C, Czerny M, Sodeck GH, Ta J, Schoder M, Funovics M, et al. A new mechanism by which an acute type B aortic dissection is primarily complicated, becomes complicated, or remains uncomplicated. *Ann Thorac Surg* 2012;**93**:1215–22.
- Tolenaar JL, van Keulen JW, Jonker FHW, van Herwaarden JA, Verhagen HJ, Moll FL, et al. Morphologic predictors of aortic dilatation in type B aortic dissection. *J Vasc Surg* 2013;**58**:1220–5.
- Sueyoshi E, Sakamoto I, Uetani M. Growth rate of affected aorta in patients with type B partially closed aortic dissection. *Ann Thorac Surg* 2009;**88**:1251–7.
- Tolenaar JL, Eagle KA, Jonker FHW, Moll FL, Elefteriades JA, Trimarchi S. Partial thrombosis of the false lumen influences aortic growth in type B dissection. *Ann Cardiothorac Surg* 2014;**3**:275–7.
- Tsai TT, Schlicht MS, Khanafer K, Bull JL, Valassis DT, Williams DM, et al. Tear size and location impacts false lumen pressure in an ex vivo model of chronic type B aortic dissection. *J Vasc Surg* 2008;**47**:844–51.
- Nienaber CA, Kische S, Rousseau H, Eggebrecht H, Rehders TC, Kundt G, et al. Endovascular repair of type B aortic dissection: long-term results of the randomized investigation of stent grafts in aortic dissection trial. *Circ Cardiovasc Interv* 2013;**6**:407–16.
- Dillon-Murphy D, Noorani A, Nordsletten D, Figueroa CA. Multi-modality image-based computational analysis of haemodynamics in aortic dissection. *Biomech Model Mechanobiol* 2016;**15**:857–76.
- Khoynezhad A, Walot I, Kruse MJ, Rapae T, Donayre CE, White RA. Distribution of intimomedial tears in patients with type B aortic dissection. *J Vasc Surg* 2010;**52**:562–8.
- Shahcheraghi N, Dwyer HA, Cheer AY, Barakat AI, Rutaganira T. Unsteady and three-dimensional simulation of blood flow in the human aortic arch. *J Biomech Eng* 2002;**124**:378–87.
- Lavingia KS, Larion S, Ahanchi SS, Ammar CP, Bhasin M, Mirza AK, et al. Volumetric analysis of the initial index computed tomography scan can predict the natural history of acute uncomplicated type B dissections. *J Vasc Surg* 2015;**62**:893–9.